HHS Public Access

Author manuscript

Br J Ophthalmol. Author manuscript; available in PMC 2020 July 16.

Published in final edited form as:

Br J Ophthalmol. 2019 January ; 103(1): 88–93. doi:10.1136/bjophthalmol-2017-311586.

Evaluation of choroidal lesions with swept-source optical coherence tomography

Cindy Ung[1], **Inês Laíns**[1,2], **Rebecca F Silverman**[1], **Russell Woods**[3], **Anne Marie Lane**[1], **Thanos D Papakostas**[1], **Deeba Husain**[1], **Joan W Miller**[1], **Evangelos S Gragoudas**[1], **Ivana K Kim**[1], **John B Miller**[1]

[1]Retina Service, Massachusetts Eye and Ear, Department of Ophthalmology, Harvard Medical School, Boston, Massachusetts, USA

[2]Faculty of Medicine, University of Coimbra, Coimbra, Portugal

[3]Department of Ophthalmology, Harvard Medical School, Schepens Eye Research Institute, Boston, Massachusetts, USA

Abstract

Aims—The aim of our study was to image choroidal lesions with swept-source optical coherence tomography (SS-OCT) and to identify the morphological characteristics associated with optimal visualisation.

Methods—This was a prospective, cross-sectional study. Patients with choroidal melanocytic lesions <3 mm in thickness on B-scan ultrasonography were recruited. All participants underwent SS-OCT. On SS-OCT we evaluated qualitative (eg, lesion outline, detection of scleral-choroidal interface and quality of the image) and quantitative (measurement of maximum lesion thickness and the largest basal diameter) parameters. Probability of optimal image quality was examined using ordered logistic regression models. The main outcome measure was quality of the choroidal lesion images on SS-OCT, defined as: optimal, suboptimal or poor.

Results—We included 85 choroidal lesions of 82 patients. There were 24 choroidal lesions (29%) for which image quality was classified as optimal, 31 lesions (37%) as suboptimal and 30 lesions (36%) as poor. The factors associated with optimal image quality were distance closer to

Correspondence to: Dr John B Miller, Retina Service, Massachusetts Eye and Ear, Department of Ophthalmology, Harvard Medical School, Boston, MA 02114, USA; john_miller@meei.harvard.edu.

CU and IL contributed equally.

Contributors IL, A-ML, DH, JWM, EG, IKK and JBM were responsible for the conception and design of this research project, as well as for obtaining the required institutional review board approval. CU, IL, RFS, A-ML, TDP, DH, JWM, EG, IKK and JBM were responsible for data collection. CU, IL, RFS, RW, TDP, JBM were responsible for images and data analysis. CU and IL drafted the manuscript, and all authors critically commented on and approved the final submitted version of the paper.

Competing interests IL receives travel expenses from Allergan. IKK: Consultant to Allergan, Alcon, Genentech and Iconic Therapeutics. JWM: Consultant to Alcon Research Institute, KalVista Pharmaceuticals Ltd, Maculogix Inc; Patent with ONL Therapeutics LLC, Royalties from Valeant Pharmaceuticals. JBM: Consultant to Allergan. The following authors have no financial disclosures: CU, RFS, RW, AML, TDP, DH, ESG.

Patient consent Detail has been removed from this case description/these case descriptions to ensure anonymity. The editors and reviewers have seen the detailed information available and are satisfied that the information backs up the case the authors are making.

Ethics approval The protocol adhered to the tenets of the declaration of Helsinki, complied with the Health Insurance Portability and Accountability Act, and was approved by the Massachusetts Eye and Ear Institutional Review Board.

Provenance and peer review Not commissioned; externally peer reviewed.

the fovea (OR 0.76, p<0.001), posterior pole location (OR 3.87, p=0.05), lower ultrasonography thickness (OR 0.44, p=0.04), lighter lesion pigmentation (OR 0.12, p=0.003) and smaller lesion diameter (OR 0.73, p<0.001). In the multivariable analysis, closer distance to the fovea (OR 0.81, p=0.005), lighter lesion pigmentation (OR 0.11, p=0.01) and smaller lesion diameter (OR 0.76, p=0.006) remained statistically significant.

Conclusion—SS-OCT is useful in imaging most choroidal melanocytic lesions. Image quality is best when the choroidal lesion is closer to the fovea, has a smaller diameter and a lighter choroidal pigmentation.

INTRODUCTION

Benign choroidal lesions can be present in up to 7.9% of the Caucasian population in the USA, and can progress to malignant uveal melanoma.[1] Currently, ultrasonography is the gold standard imaging modality for characterising choroidal lesions. However, it has limited resolution for evaluating smaller thickness lesions,[2] and requires a trained ultrasonographer, which can limit patient access in certain clinical settings.

Recent advances in optical coherence tomography (OCT) have made it a valuable tool in assessing choroidal lesions. Older OCT versions provided little detail within the lesions or surrounding choroid.[3] Spaide *et al*[4] introduced the enhanced depth imaging (EDI) protocol for spectral domain (SD)-OCT, which provided improved visualisation.[5] However, this technique may be limited by shadowing and result in poor image resolution.[5]

A significant, recent development in ocular imaging was the swept-source OCT (SS-OCT). SS-OCT uses a wavelength-sweeping laser of 1050 nm as the light source, providing greater tissue depth than previous OCT systems. Early studies have demonstrated the improved ability of SS-OCT to image deep ocular structures in different diseases.[6–8] Francis *et al*[9] showed that SS-OCT was significantly better at depicting intralesional characteristics of choroidal lesions compared with other OCT techniques.

Although groups have looked at the characteristics of choroidal lesions on SS-OCT, no study has evaluated lesion-related characteristics for ideal SS-OCT imaging.[9–11] The aim of this study was to assess the ability of SS-OCT to image choroidal lesions, and to identify the morphological characteristics associated with optimal visualisation.

METHODS

This was a prospective, observational, cross-sectional study. Written informed consent was obtained from all participants prior to enrolment in the study.

Participants and imaging protocol

Patients with the diagnosis of a pigmented choroidal lesion <3 mm in thickness on ultrasonography were prospectively enrolled from the retina clinic at Massachusetts Eye and Ear from August 2014 to October 2015. We excluded subjects with media opacity that precluded proper imaging and subjects with the diagnosis of choroidal melanoma. We enrolled 82 patients of the 95who were eligible (86%). All enrolled subjects received a

complete ophthalmological examination, including best-corrected visual acuity, intraocular pressure, dilated fundus examination and ultrasonography. Cataract status was based on the WHO simplified cataract grading system.[12] All participants underwent colour fundus photography (Topcon TRC-50DX, Topcon Corporation, Tokyo, Japan). On the same visit, SS-OCT imaging was performed with DRI Atlantis OCT (Topcon Medical Systems, Oakland, New Jersey, USA). SS-OCT images were obtained after pupillary dilatation in all patients. We used a scanning protocol available on the commercial device, which consisted of a 3D horizontal volume (12 mm × 9 mm) and a radial protocol (12 lines) over the choroidal lesion.

Data collection and imaging assessment

Demographic data recorded for each patient included gender, age, past medical history and presence of symptoms at presentation. The features recorded on standard ultrasonography included height (millimetres), maximal basal diameter (millimetres) and location of the lesion.

Two independent graders (CU, IL) assessed choroidal lesions on colour fundus photos using IMAGEnet 2000 software V.2.56 (Topcon Medical Systems) for the presence of drusen, lipofuscin and degree of pigmentation. Three grades of choroidal lesion pigmentation were used:[13] light (large choroidal vessels appear darker than the choroid due to minimal pigmentation between vessels), medium (large choroidal vessels are difficult to distinguish from the choroid due to patchy or incomplete choroidal pigmentation) and dark (large choroidal vessels appear lighter than, and stand out against, the dark choroidal pigment between the vessels). In cases of disagreement, the final decision was made by the senior author (JBM). Using the same software, the two graders independently used digital callipers to record the distance of nearest lesion margin to optic disc margin and fovea (in millimetres). Mean data were used for analysis. In cases where discrepancies in measurements were ≥5% (n=1), the senior author (JBM) measured the same parameters, and his measurement was included for determination of the mean.

Evaluation of SS-OCT images

SS-OCT images were analysed by the same two graders (CU, IL), who assessed various morphological parameters after a review of the literature.[5914] For each lesion, the following features were evaluated: presence or absence of intraretinal fluid, subretinal fluid and drusen above the lesions; visualisation of the ellipsoid zone above the lesions (yes vs no); visualisation of the posterior and/or anterior limit of the lesions (yes vs no); visualisation of scleral-choroidal interface (clearly visible; possible to imagine but not clearly visible; not visible); type of inner reflectivity (high if reflectivity was similar to retinal pigment epithelium (RPE) vs intermediate if reflectivity is between RPE and vitreous); and presence of intralesional vessels or cavities (yes vs no). Characteristics of lesion configuration, visibility of choriocapillaris above the lesion, vessels within lesion, cavities within lesion and hyporeflective gradation of lesion-scleral interface were only analysed in optimal and suboptimal images, as these features require good quality images to appreciate these details. The configuration of the lesions was categorised as: plateau (no distention of the retina), dome (distention of retina only), almond (distention of the retina and sclera) and no

distention of the retina or choroid.[9] Quantitative analysis comprised measuring the maximum lesion thickness from the hyper-reflective line corresponding to the Bruch membrane/RPE junction to the inner sclera and measurement of the largest lesion diameter using the calliper tool within the SS-OCT instrument. For these quantitative parameters, the mean of the measurements obtained by the two graders was used for calculations. In cases where discrepancies were ≥5% the senior author measured the same parameters (n=3), and his results were included for determination of the average.

Finally, the same two graders evaluated all SS-OCT images for image quality: optimal (all margins of the lesion well visible), suboptimal (at least one margin not properly imaged) or poor (more than one margin not properly imaged). Examples are seen in figure 1. In cases of disagreement, the senior author established the final categorisation.

Statistical analysis

Data were analysed using Stata V.14.1 (Stata Corporation, College Station, Texas, USA). Possible differences between image-quality groups were analysed using Pearson's χ^2 test, the Kruskal-Wallis test, the non-parametrical trend test and ordered logistic regression (OLR). Agreement between the two graders for imaging features assessed as binomial and dichotomous variables (both on colour fundus photographs and SS-OCT) was calculated using κ statistics, where a κ value of 1 indicates perfect agreement and 0 an agreement by chance.[15]

A multiple (multivariable) OLR (that started with the terms that showed differences between image-quality groups in univariate OLR) was used to develop a model of predictors of image quality. A backward-stepwise approach for removal of non-significant ($p>0.10$) terms was followed. There were three subjects who contributed more than one lesion to the study. Alternative analyses that included only one lesion from each of those three subjects did not produce analysis outcomes that differed substantively from analyses that included all lesions, so we report analyses with all lesions.

RESULTS

Included study population

We included 85 choroidal lesions of 82 patients, mean age 65.8±11.8 years; 34 (41%) were male and 48 (59%) were female. There were three patients who contributed two lesions each; two patients had two lesions in one eye, and one patient had one lesion in each eye.

As assessed on SS-OCT of the 85 choroidal lesions, the quality of the image was judged to be optimal in 24 lesions (29%), suboptimal in 31 (37%) and poor in 30 (36%). Characterisation of imaged eyes is described in table 1. Inter-rater agreement for the imaging features assessed varied between 89% and 100%, $\kappa \geq 0.8$ ($p \leq 0.001$ for all).

Lesions with optimal image quality were more likely to be located in the posterior pole ($p=0.005$) or closer to the fovea ($p<0.001$), to have a smaller diameter ($p<0.001$), lighter pigmentation ($p=0.001$) or smaller lesion thickness as measured by ultrasonography

(p=0.04). The presence of cataract was not significantly associated with image quality (p=0.101).

Image quality data

Table 2 presents the SS-OCT characteristics of choroidal lesions, as assessed by the two graders. The lesion posterior limit, anterior limit and scleral-choroidal interface were less likely to be visible in lesions with poor image quality (all p<0.001). Characteristics including high inner reflectivity and high reflectivity with posterior shadowing were more likely to be seen in poor quality images (p<0.001). As detailed in the Methods section, lesion configuration, visibility of choriocapillaris above the lesion, vessels within lesion, cavities within lesion and hyporeflective gradation of lesion-scleral interface were only analysed in optimal and suboptimal images, as these features require good quality images to grade these characteristics. Of the 55 lesions with suboptimal and optimal image quality, hyporeflective gradation of lesion-scleral interface was found to be statistically different between them (p=0.005). There were no significant differences in lesion thickness on SS-OCT between image-quality groups.

Variables associated with SS-OCT images quality

All the evaluated potential predictors of optimal image quality are shown in table 3. In univariable OLR analyses, the factors associated with optimal image quality were closer distance to the optic nerve head (OR 1.12, p=0.05), closer distance to the fovea (OR 1.31, p<0.001), posterior pole location (OR 3.87, p=0.003), lower ultrasonography thickness (OR 2.27, p=0.04), lighter pigmentation (OR 8.33, p=<0.01) and smaller maximum lesion diameter (OR 1.37, p<0.001). All variables found significant in those univariable analyses were included in an initial multivariable ordered logistic regression. Following backwards-stepwise removal, the significant independent predictors of SS-OCT image quality were smaller distance to the fovea (p<0.001), lighter lesion pigmentation (p=0.01) and smaller maximum lesion diameter (p=0.006).

As the current gold standard for measurement of choroidal lesion thickness is ultrasonography, we explored its relationship with the values obtained with SS-OCT. Thickness measured with ultrasonography was correlated with that measured with SS-OCT (Spearman's r=0.77, p<0.001). Mean lesion thickness by ultrasonography was 1020±550 μm (range, 500–3000 μm) and by SS-OCT imaging it was 636.8±371.2 μm (range: 119–1676 μm). The mean difference between the measurements of lesion thickness on ultrasonography and SS-OCT was 236.0±277.7 μm (range: −205–1205 μm), which was statistically significant (Z-value=−5.4293, p<0.01).

DISCUSSION

We prospectively recruited 82 patients with 85 choroidal lesions to identify factors that were related to SS-OCT image quality. This device enabled optimal or suboptimal imaging for the majority of the lesions (n=55; 65.5%). Multiple regression analysis revealed that smaller distance to the fovea, lighter pigmentation and smaller maximum lesion diameter were significant independent predictors of better imaging quality.

While there have been several studies looking at SS-OCT of choroidal lesions,[9–11] to our knowledge, characteristics of choroidal lesions that relate to optimal image quality with SS-OCT have not been evaluated. Prior studies have recognised the influence of pigmentation on image quality and characteristics.[5] In our study, three grades of pigmentation of the lesions were assessed: light, medium and dark.[13] We found that increased pigmentation was associated with poor quality images. Dark pigmentation reflects an increase in density of choroidal melanocytes and the poor quality images are likely related to the presence of light-reflecting/scattering melanin.[14]

Our study also showed that choroidal lesions located outside the posterior pole were associated with poor image quality, probably because it is difficult to image lesions with a more peripheral location. Additionally, lesions located an average of 8 mm away from the fovea (representing mid-periphery) were more likely to have poor quality. Most of our lesions were located closer to the fovea (with 29 lesions in the macula), which is in agreement with prior data.[16]

Several studies have looked at the intralesional characteristics of choroidal lesions on SS-OCT, including details such as vessels, cavities and granularity.[9] These have found improved visualisation of the inner structures in a series of choroidal tumours.[1011] In our study, there was no difference in visualisation of the choriocapillaris, vessels within lesion, and cavities within lesion between optimal and suboptimal images. However, optimal images were also more likely to show hyporeflective gradation of lesion-scleral interface compared with poor images. This gradation has been thought to be due to the transition of polyhedral cells in the inner portion of the lesion transitioning to densely packed spindle cells in the scleral interface.[9]

Ultrasonography is historically the most used imaging modality for evaluating intraocular lesions. Previous studies have identified differences between ultrasonography and OCT measurement of lesion thickness.[17] In our study, we noted a similar difference in the choroidal lesion thickness measured by ultrasonography (mean, 1.02 mm) versus SS-OCT (mean, 0.64 mm), with a 37.5% lower measurement with SS-OCT. This may be a more precise measurement with SS-OCT, given better resolution of the choroidal-scleral interface.[8] Ultrasonography may overestimate lesion thickness by including the overlying retina or the underlying sclera.[18] The axial resolution of SS-OCT allows for more precise measurements of select lesions.[19] This may allow for more accurate longitudinal monitoring of interval thickness changes and may help with earlier detection of malignant transformation. The ability to monitor premalignant choroidal lesions by SS-OCT could be a valuable clinical tool, providing greater patient access to disease monitoring in underserved communities without a trained ultrasonographer.

We recognise some limitations of this study. Our cases were from a single institution in a referral centre setting, which may not be representative of the population at large. While it is one of the largest series on choroidal lesions, the sample size is still limited, and the results may not be generalisable. The measurement of lesion thickness and evaluation of some characteristics was difficult in lesions with poor image quality. The missing data for these lesions may have led to bias. Despite our high rate of intergrader agreement, in cases of

disagreement, the senior author assessment was considered. This approach has limitations, and forced adjudication could have been another option. This study also offers a single time point assessment of choroidal lesions. Future work is required with prospective studies to assess the ability of SS-OCT to monitor changes in choroidal lesions over time.

In summary, SS-OCT allows for improved visualisation of choroidal lesions. Axial resolution of SS-OCT is better than ultrasonography and highlights the potential to monitor these lesions with continued improvements in OCT technology. We were able to identify characteristics of choroidal lesions that affect optimal image quality with SS-OCT. Our results revealed that image quality decreases with increasing distance of the edge of the choroidal lesion from the fovea, increasing lesion thickness as measured with ultrasonography, darker pigmentation and larger lesion diameter. These findings are comparable with that of a prior study that found that image quality of nevi with EDI-OCT decreased with extramacular location and increasing lesion diameter.[17] Despite some limitations, the technique itself provides high-resolution, non-invasive visualisation of choroidal lesions without the need for a trained ultrasonographer. These results highlight the potential increasing application of SS-OCT to assess choroidal lesions in the future.

Funding

The Miller Retina Research Fund (Mass. Eye and Ear); the Miller Champalimaud Vision Award (Mass. Eye and Ear) (to JWM); Portuguese Foundation for Science and Technology/Harvard Medical School Portugal Programme (HMSPICJ/006/2013) (to IL); Ronald G. Michels Foundation (to TDP).

REFERENCES

1. Singh AD, Kalyani P, Topham A. Estimating the risk of malignant transformation of a choroidal nevus. Ophthalmology 2005;112:1784–9. [PubMed: 16154197]
2. Chien JL, Sioufi K, Surakiatchanukul T, et al. Choroidal nevus: a review of prevalence, features, genetics, risks, and outcomes. Curr Opin Ophthalmol 2017;28:228–37. [PubMed: 28141766]
3. de Bruin DM, Burnes DL, Loewenstein J, et al. In vivo three-dimensional imaging of neovascular age-related macular degeneration using optical frequency domain imaging at 1050 nm. Invest Ophthalmol Vis Sci 2008;49:4545. [PubMed: 18390638]
4. Spaide RF, Koizumi H, Pozzoni MC, et al. Enhanced depth imaging spectral-domain optical coherence tomography. Am J Ophthalmol 2008;146:496–500. [PubMed: 18639219]
5. Torres VL, Brugnoni N, Kaiser PK, et al. Optical coherence tomography enhanced depth imaging of choroidal tumors. Am J Ophthalmol 2011;151:586–93. [PubMed: 21257150]
6. Laíns I, Talcott KE, Santos AR. Choroidal thickness in diabetic retinopathy assessed with swept-source optical coherence tomography. Retina 2017;1.
7. Ohno-Matsui K, Akiba M, Ishibashi T, et al. Observations of vascular structures within and posterior to sclera in eyes with pathologic myopia by swept-source optical coherence tomography. Invest Ophthalmol Vis Sci 2012;53:7290–8. [PubMed: 23033385]
8. Adhi M, Liu JJ, Qavi AH, et al. Enhanced visualization of the choroido-scleral interface using swept-source OCT. Ophthalmic Surg Lasers Imaging Retina 2013;44(6 Suppl):S40–S42.
9. Francis JH, Pang CE, Abramson DH, et al. Swept-source optical coherence tomography features of choroidal nevi. Am J Ophthalmol 2015;159:169–76. [PubMed: 25448319]
10. Michalewska Z, Michalewski J, Nawrocki J. Swept Source optical coherence tomography of choroidal nevi. Can J Ophthalmol 2016;51:271–6. [PubMed: 27521666]
11. Filloy A, Caminal JM, Arias L, et al. Swept source optical coherence tomography imaging of a series of choroidal tumours. Can J Ophthalmol 2015;50:242–8. [PubMed: 26040226]

12. Thylefors B, Chylack LT, Konyama K, et al. A simplified cataract grading system. Ophthalmic Epidemiol 2002;9:83–95. [PubMed: 11821974]
13. Harbour JW, Brantley MA, Hollingsworth H, et al. Association between choroidal pigmentation and posterior uveal melanoma in a white population. Br J Ophthalmol 2004;88:39–43. [PubMed: 14693770]
14. Shields CL, Mashayekhi A, Materin MA, et al. Optical coherence tomography of choroidal nevus in 120 patients. Retina 2005;25:243–52. [PubMed: 15805899]
15. Viera AJ, Garrett JM. Understanding interobserver agreement: the kappa statistic. Fam Med 2005;37:360–3. [PubMed: 15883903]
16. Shields CL, Furuta M, Mashayekhi A, et al. Clinical spectrum of choroidal nevi based on age at presentation in 3422 consecutive eyes. Ophthalmology 2008;115:546–52. [PubMed: 18067966]
17. Shah SU, Kaliki S, Shields CL, et al. Enhanced depth imaging optical coherence tomography of choroidal nevus in 104 cases. Ophthalmology 2012;119:1066–. [PubMed: 21943786]
18. Witkin AJ, Fischer DH, Shields CL, et al. Enhanced depth imaging spectral-domain optical coherence tomography of a subtle choroidal metastasis. Eye 2012;26:1598–9. [PubMed: 23037908]
19. Mrejen S, Spaide RF. Optical coherence tomography: imaging of the choroid and beyond. Surv Ophthalmol 2013;58:387–429. [PubMed: 23916620]

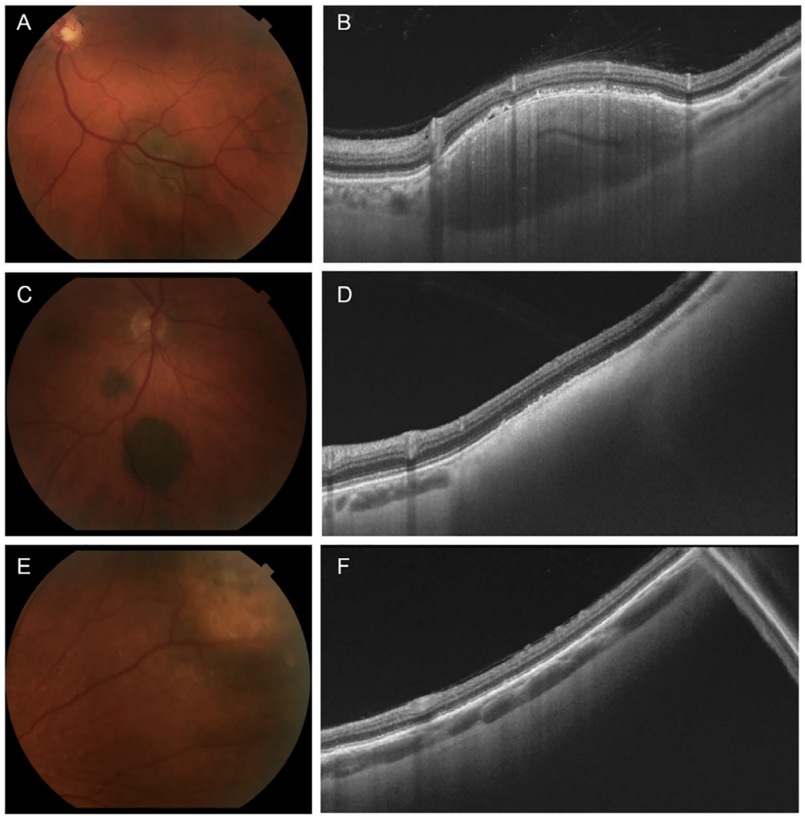

Figure 1.

Fundus photographs and swept-source optical coherence tomography (SS-OCT) of choroidal lesions. (A) Color fundus photograph of choroidal lesion with medium pigmentation. (B) SS-OCT image of choroidal lesion in A with optimal image quality and an almond configuration demonstrating intralesional vessels and heterogenous reflectivity. (C) Color fundus photograph of choroidal lesion with dark pigmentation. (D) SS-OCT image of choroidal lesion in C with suboptimal image quality and high posterior shadowing which compromised visualisation of the sclerochoroidal interface. (E) Color fundus photograph of peripheral choroidal lesion. (F) SS-OCT image of choroidal lesion in E with poor image quality.

Table 1

Demographic and clinical features of the imaged eyes, according to swept-source optical coherence tomography image quality

	Optimal (n=24)	Suboptimal (n=31)	Poor (n=30)	P values
Median age (years) (range)	67 (24–88)	67 (53–91)	66.5 (39–88)	0.94
Gender				
Male	13 (54%)	13 (42%)	9 (30%)	0.21
Female	11 (46%)	18 (58%)	21 (70%)	
Eye				
Left	14 (58%)	14 (45%)	17 (57%)	0.56
Right	10 (42%)	17 (55%)	13 (43%)	
Symptoms				
None	18 (75%)	18 (58%)	21 (70%)	0.40
Present	6 (25%)	13 (42%)	9 (30%)	
Median visual acuity of affected eye (logMAR), (range)	0.0 (–0.12–0.18)	0.0 (–0.12–0.54)	0.0 (–0.12–0.5)	0.29
Cataract	8 (33%)	13 (42%)	19 (63%)	0.08
1 +	6 (25%)	10 (32%)	16 (53%)	
2+	1 (4%)	3 (10%)	3 (10%)	
3+	1 (4%)	0 (0%)	0 (0%)	
Median IOP (mm Hg) (range)	14 (9–22)	17 (12–22)	15 (10–21)	0.28
Choroidal lesion pigmentation				
Light	7 (29%)	2 (6%)	2 (7%)	0.001
Medium	9 (38%)	19 (61%)	6 (20%)	
Dark	8 (33%)	10 (32%)	22 (73%)	
Posterior pole location				
Yes	12 (50%)	13 (42%)	3 (10%)	0.005
No	12 (50%)	18 (58%)	27 (90%)	
Location based on fundus photos				
Inferior	7 (29%)	10 (33%)	12 (40%)	0.70
Temporal	10 (42%)	11 (37%)	10 (33%)	0.90
Superior	4 (17%)	4 (13%)	8 (27%)	0.33
Nasal	3 (13%)	5 (17%)	11 (37%)	0.05

	Optimal (n=24)	Suboptimal (n=31)	Poor (n=30)	P values
Peripapillary	1 (4%)	2 (7%)	4 (13%)	0.45
Macula	11 (46%)	14 (47%)	4 (13%)	0.015
Median distance from the optic disc (mm) (range)	4.8 (0–8.0)	3.5 (0–13.6)	5.9 (0–14.6)	0.11
Median distance from the fovea (mm) (range)	3.0 (0.2–10.0)	3.3 (0–12.0)	7.4 (0–18.6)	<0.001
Drusen				
No	9 (37%)	4 (13%)	4 (13%)	0.05
Yes	15 (63%)	27 (87%)	26 (87%)	
Lipofuscin				
No	22 (92%)	23 (74%)	23 (77%)	0.25
Yes	2 (8%)	8 (26%)	7 (23%)	
Median maximum lesion diameter (mm) (range)	4.3 (1.7–10.9)	5.1 (1.8–10.9)	7.0 (3.2–18.1)	<0.001
Median lesion thickness by ultrasonography (mm) (range)	<1 (<1–2.1)	1 (<1–1.8)	1.25 (<1–3)	0.04

IOP, intraocular pressure.

Table 2

Swept-source optical coherence tomography characteristics of the imaged choroidal lesions, according to image quality

	Optimal (n=24)	Suboptimal(n=31)	Poor (n=30)	P values
Intraretinal fluid				
Absent	20 (83%)	26 (87%)	10 (45%)	0.89
Present	4 (17%)	4 (13%)	4 (13%)	
Subretinal fluid				
Absent	9 (37%)	9 (30%)	5 (17%)	0.57
Present	15 (63%)	21 (67%)	17 (57%)	
Drusen				
Absent	6 (25%)	6 (19%)	3 (10%)	0.60
Present	18 (75%)	24 (77%)	20 (67%)	
Ellipsoid zone				
Disrupted	18 (75%)	24 (77%)	20 (67%)	0.38
Normal	6 (25%)	6 (19%)	2 (7%)	
Visibility of posterior limit				
Absent	0	1 (3%)	9 (30%)	<0.001
Present	24 (100%)	30 (97%)	21 (70%)	
Visibility of anterior limit				
Absent	0	6 (19%)	20 (67%)	<0.001
Present	24 (100%)	25 (81%)	10 (33%)	
Visibility of scleral-choroidal interface				
No	0	10 (32%)	30 (100%)	<0.001
Possible	2 (8%)	15 (48%)	0	
Yes	22 (92%)	6 (19%)	0	
Inner reflectivity				
Intermediate	20 (83%)	9 (30%)	3 (10%)	<0.001
High	4 (17%)	22 (70%)	22 (73%)	
Type of reflectivity				
High with posterior shadowing	1 (4%)	10 (32%)	21 (70%)	<0.001
Heterogeneous	16 (67%)	15 (48%)	1 (3%)	
Homogenous	7 (29%)	6 (19%)	3 (10%)	
Lesion configuration *				
No distention	5 (21%)	7 (23%)		0.21
Almond	12 (50%)	14 (45%)		
Dome	4 (17%)	7 (23%)		
Plateau	3 (13%)	0		
Choriocapillaries visible above lesion *				
Absent	10 (42%)	19 (61%)		0.16
Present	14 (58%)	12 (39%)		
Vessels within lesion *				

	Optimal (n=24)	Suboptimal(n=31)	Poor (n=30)	P values
Absent	18 (75%)	28 (90%)		0.14
Present	6 (25%)	3 (10%)		
Cavities within lesion *				
Absent	23 (96%)	31 (100%)		0.26
Present	1 (4%)	0		
Hyporeflective gradation of lesion-scleral interface *				
Absent	12 (50%)	27 (87%)		0.005
Present	12 (50%)	4 (13%)		
Median choroidal thickness (μm) * (range)	503 (119–1,676)	608 (214–1,371)		0.88
Maximum lesion width (mm) * (range)	5.11 (1.49–11.03)	4.90 (0.92–7.63)		0.69

* Only lesions with optimal and suboptimal image quality were analysed.

Table 3

Ordinal logistic regression analyses of predictors of optimal image quality

	Univariable ordinal logistic regression			Multivariable ordinal logistic regression (significant terms only)		
Variable	**or**	**95% CI**	**P values**	**or**	**95% CI**	**P values**
Distance to the optic nerve head	0.89	0.79 to 1.00	0.05	–	–	–
Distance to the fovea	0.76	0.68 to 0.88	<0.001	0.78	0.68 to 0.90	0.005
Choroidal pigmentation						
Dark versus light	0.12	0.03 to 0.48	0.003	0.12	0.20 to 0.62	0.01
Dark versus medium	0.31	0.13 to 0.77	0.01	1.11	0.39 to 3.32	0.86
Medium versus light	0.37	0.09 to 1.48	0.16	0.11	0.02 to 0.65	0.01
Posterior pole location	3.87	1.60 to 9.40	0.003	–	–	–
Thickness measured using ultrasonography	0.44	0.20 to 0.96	0.04	–	–	–
Thickness measured using SS-OCT	1.00	1.00 to 1.00	0.84	–	–	–
Maximum diameter	0.73	0.61 to 0.87	<0.001	0.76	0.62 to 0.92	0.006

SS-OCT, swept-source optical coherence tomography; OR, odds ratio.